3D morphological reconstruction of the red blood cell based on two phase images

Yawei Wang[1, 2], Li Zhang[1], Ying Ji[2*], Yuanyuan Xu[1], Min Bu[2], Yingzhou Chen[2]

[1]School of Mechanical Engineering, Jiangsu University, Zhenjiang 212013, China

[2]Faculty of Science, Jiangsu University, Zhenjiang 212013, China

*Corresponding author: jy@ujs.edu.cn

As an important component of blood cells, the red blood cell plays a vital role in many diseases such as malaria and so on. Although quantitative phase imaging techniques can be used for homogeneous cellular thickness distribution to obtain ideal results, they cannot achieve 3D morphological distribution. In this paper, a new method is presented to get a 3D morphology image of red blood cell. With this method, only two cellular quantitative phase images obtained from two orthogonal directions are needed as original information. By using the grid method, the sample is divided into many small phase cubes, and then we take a layer's cubes into calculation so that the 3D problem could be transformed into a 2D problem to elaborate. Then it can be applied to the tomographic imaging combined with the maximum entropy method according to the two orthogonal phase images. This method has been proved by a simulation of red blood cell. The results show that cellular morphological distribution can be achieved in detail very well just based on only two orthogonal phase images.

Keywords: phase imaging, red blood cell, 3D morphological reconstruction, maximum entropy.

1. Introduction

In the human blood, the largest numbers of blood cells are red blood cells (RBC). Research on the morphology of RBC is significant to human health. A series of blood diseases can be diagnosed by detecting the abnormal changes in red blood cell morphology, such as autoimmune hemolytic and sickle cell anemia. However, the 3D morphological distribution of RBC is hard to be obtained by traditional optical microscopy due to the transparent property of RBC. To solve this problem, several methods have been proposed, such as phase contrast and differential interference contrast based on the phenomenon of the optical path-length shifts across the specimen. Unfortunately, only qualitative information can be obtained by these techniques.

Over the last decades, significant progress has been made in quantitative phase imaging (QPI) methods [1, 2] which promise to overcome the limitation of traditional phase microscopy. Various techniques have been proposed for studying the transparent biological specimens [3], including the Fourier phase microscopy (FPM) [4], the Hilbert phase microscopy (HPM) [5], the diffraction phase microscopy (DPM) [6], the asynchronous digital holography (ADH) [7] and so on. QPI technique becomes one of the main technologies applied to study microscopic structure and dynamics behavior of biological cells because of the advantages of its high sensitivity, high sampling rate, high accuracy and non-intrusive method without injury. However, the traditional QPI can only obtain the biological cells' thickness distribution. Some recent progress has been made to discover the 3D morphological distribution of biological cells [8–11], such as optical diffraction tomography [12–15] and marker-free phase nanoscopy [16].

In order to explore cellular morphology, a new tomography [17–19] entropy method of 3D imaging based on orthogonal phase images has been presented in this paper. This approach only needs the cellular quantitative phase information in two orthogonal directions as input data, rather than holograms with various illumination angles (from –60 deg to +60 deg), and can be obtained from the 3D refractive index distribution by using this iterative algorithm; furthermore it reconstructs the 3D morphology information. This method is based on fast convergence and high efficiency of the maximum entropy reconstruction method, and it only needs quantitative phase information on the cell in two orthogonal directions which could reduce the amount of data calculation. This advantage makes this method very suitable for tomography imaging of computing refractive index distribution. In order to demonstrate the effectiveness of the method, RBC is taken as a simulation example.

2. Basic principle and method

In this method, for the sake of the determination of the cellular morphology, one should work out the spatial refractive index distribution of the phase object. For this purpose, the grid method [20–23] is applied to divide the sample into many small cubes and the cube grid should completely cover the phase object. Thus the 3D problem could be transformed into a 2D problem to elaborate by taking one layer of cube grids as a research object. The grids are composed of the serial number on the basis of a TV scan order. The grid is set as a square with k rows and k columns. The total number of the parallel light is $M = 2k$ and the total number of small squares is $N = k^2$ in the grid plane. From two orthogonal directions the cell is irradiated by parallel light, as shown in Fig. 1.

Because of biological cells' characteristics of colorless, transparent, weak absorption and scatter, the assumption of the light projection [24] can be applied to the method. So the diffraction of light in a biological sample can be negligible, and light is assumed to propagate along straight lines. The light passes through the grid and gets a phase point φ_i on the CCD, where a_{ij} is the length of the i-th scan line truncated by
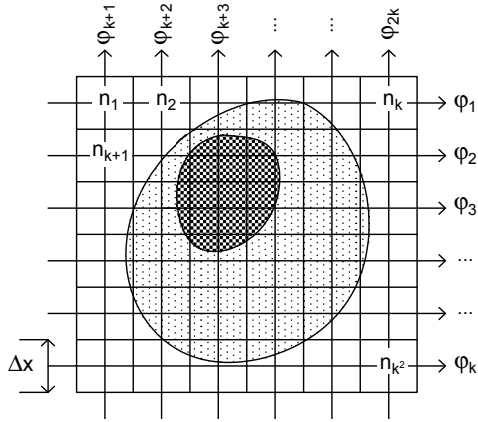
Fig. 1. 2D grid model schematic diagram.

the j-th grid element and n_j is the refractive index difference between the j-th grid element and the surrounding liquid medium. So φ_i can be given by

$$\varphi_i = \frac{2\pi}{\lambda} \sum_j a_{ij} n_j, \qquad i = 1, 2, ..., M; \quad j = 1, 2, ..., N \tag{1}$$

Since the grid is generally relatively dense, *i.e.* $M < N$, so in theory equations have infinite solutions. In order to find the optimal solution, the method of maximum entropy [25–28] is adopted.

When point (x, y) is located within a region D of an area S, entropy is defined as

$$\eta(n) = -\iint_D |n(x, y)| \ln\left[|n(x, y)|S\right] dx\, dy \tag{2}$$

Its discrete form can be rewritten into

$$\eta(n) = -\Delta x\, \Delta y \sum_j n_j \ln(S n_j), \quad j = 1, 2, ..., N \tag{3}$$

Adopting the Lagrange multiplication and attaching the boundary value conditions of the refractive index of the cell, the optimal solution can be determined by the following equation:

$$\min\{J(n_1, n_2, ..., n_N)\} = \left\{ \min \Delta S \sum_j n_j \ln(S n_j) + \gamma \sum_i \left[\phi_i - \frac{2\pi}{\lambda} \sum_j a_{ij} n_j \right]^2 \right\},$$

$$a \le n_j \le b, \quad i = 1, 2, ..., M; \quad j = 1, 2, ..., N \tag{4}$$

where $\Delta S = \Delta x \Delta y$ is the area element, ϕ_i is the phase shift that the i-th light has passed through the sample in fact, $\frac{2\pi}{\lambda} \sum_j a_{ij} n_j$ is the phase shift that the i-th light passed through the sample can be calculated by the grid method, γ is the Lagrange multiplication factor, $\gamma \sum_i \left[\phi_i - \frac{2\pi}{\lambda} \sum_j a_{ij} n_j \right]^2$ is a constraint condition, a and b are the lower and upper refractive index values, which can be appropriately selected according to the actual situation of the sample.

For a given factor γ, there is no explicit solution in Eq. (4), unless applying an iterative method to search for the optimal solution. The steepest decline in the optimization method is chosen to search for the minimum point of the objective function $J(n)$ in the negative gradient direction. The two main formulas are used.

First, the gradient of the objective function in any of a grid element can be given by

$$q_j^{(t)} = \frac{\partial J}{\partial n_j^{(t)}} = \Delta S \left[1 + \ln(S n_j^{(t)}) \right] - \frac{4\pi\gamma}{\lambda} \sum_i \left[\phi_i - \frac{2\pi}{\lambda} \sum_j n_j^{(t)} a_{ij} \right] a_{ij},$$

$$i = 1, 2, ..., M; \quad j = 1, 2, ..., N \tag{5}$$

Second, the recurrence formula of the iterative solution can be expressed as

$$n^{(t+1)} = n^{(t)} - \rho^* q^{(t)} \tag{6}$$

where $n_j^{(t)}$ is the t-th iteration solution of the j-th grid element, $n^{(t)}$ is the t-th iteration solution of all grids on the layer, $q^{(t)}$ is the t-th gradient distribution of all grids on the layer, ρ^* is the optimal step length. When function $J(n)$ takes the minimum value, the corresponding step length is the optimal step length.

When the iterative solution meets the accuracy requirements, it is outputted, which represents the difference value distribution of the refractive index between all grids and the surrounding liquid medium on the layer. Coupled with the refractive index of the surrounding liquid medium, the refractive index distribution on the layer is obtained. In the refractive index distribution, the value is denoted by n_e in the neighborhood of the refractive index of the surrounding liquid medium and the other value is denoted by $\overline{n}_c$. Thus, one can get the distribution information of the refractive index on the layer.

From the above method of calculating the refractive index distribution information of each layer, the spatial distribution of the refractive index and the physical thickness of the cell can be finally obtained. Then, the cellular 3D morphological distribution can be determined by extracting position information of the critical point between the surrounding liquid medium and the cell.

3. Simulation and results analysis

To verify the effectiveness of the method on a homogeneous cell, RBC is taken as an example. The approximate RBC model is established, and the parameters of the cross-section of the RBC model and the three-dimensional RBC model are shown in Fig. 2. In addition, the refractive index value of the surrounding liquid medium and the cell is 1.34 and 1.41, respectively [29], and the wavelength of source is set to 632.8 nm.
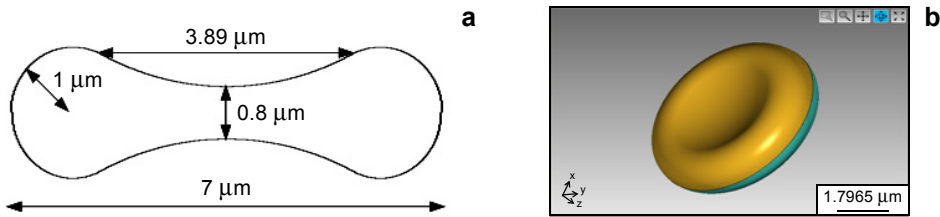
Fig. 2. The cross-section image of RBC model (**a**). The established three-dimensional RBC model (**b**).
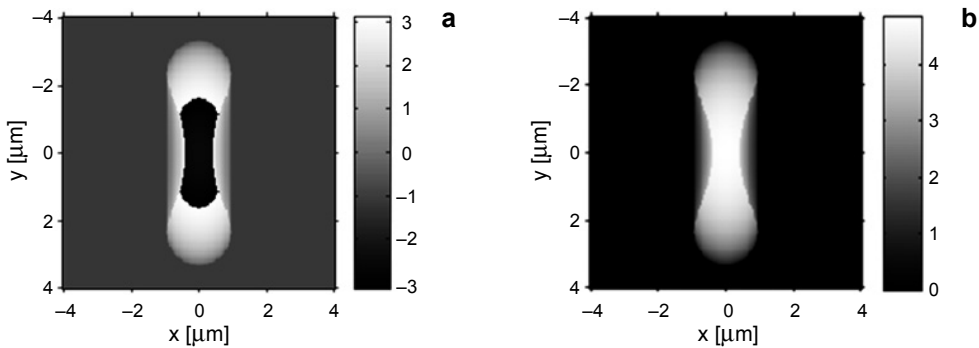
Fig. 3. The light propagates along *y*-axis. The wrapped (**a**) and unwrapped (**b**) phase image.
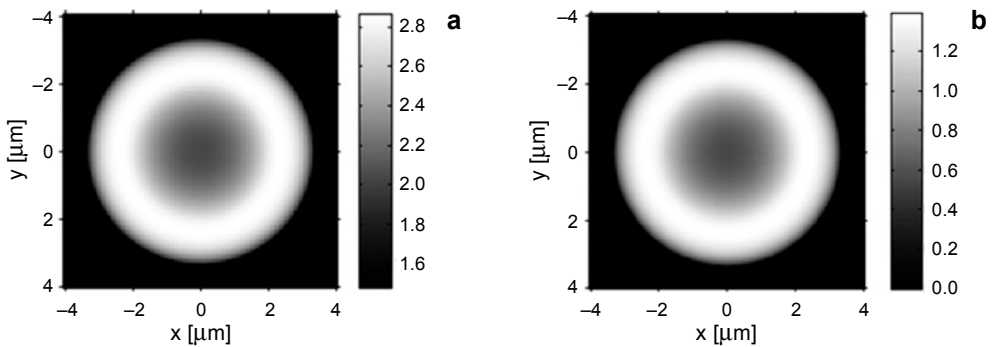
Fig. 4. The light propagates along *z*-axis. The wrapped (**a**) and unwrapped (**b**) phase image.

When RBC is parallelly irradiated by the light source from two orthogonal directions, the corresponding wrapped phase images and unwrapped phase images are acquired along the *y*-axis illumination as shown in Fig. 3 and along the *z*-axis illumination as shown in Fig. 4.

According to the methods described above, the cellular refractive index distribution information of each layer is acquired by means of MATLAB software, which is stored in a three-dimensional matrix. The cellular surface morphology information can be extracted from the matrix, especially, the coordinate information of the critical point between the surrounding liquid medium and the cell. The extracted three-dimensional discrete points can be outputted and revealed as shown in Fig. 5. Besides, the two-dimensional scatter plot of the cross-section image is demonstrated in Fig. 6.

The morphology of a concave disc shown in Fig. 5 agrees with the appearance of RBC very well. The reconstructed cross-section image of a RBC model (shown in Fig. 6) is in conformity with the shape of the model (shown in Fig. 2**a**). From which, the 3D reconstruction of RBC, including the unique biconcave disc-shape, is proved effectively. To be specific, the diameter of the reconstructed RBC is 7.10 μm and the thickness of the thinnest place is 0.84 μm, with the corresponding errors at 1.4% and 5.5%, respectively.
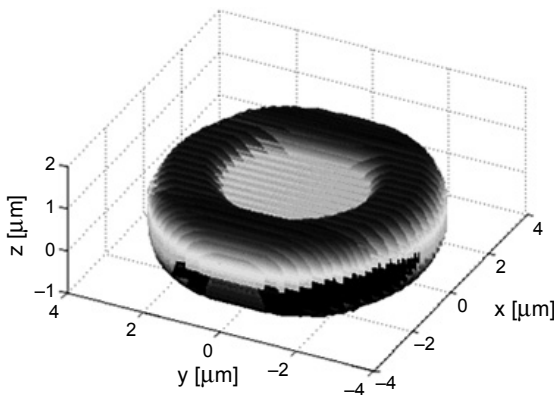

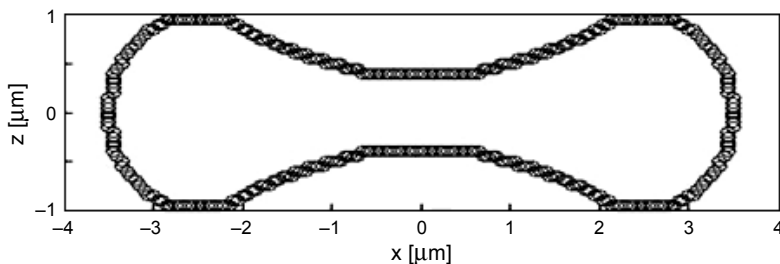Fig. 5. 3D morphological distribution of RBC.

Fig. 6. Scatter plot of the reconstructed cross-section image of 3D morphological distribution of RBC.
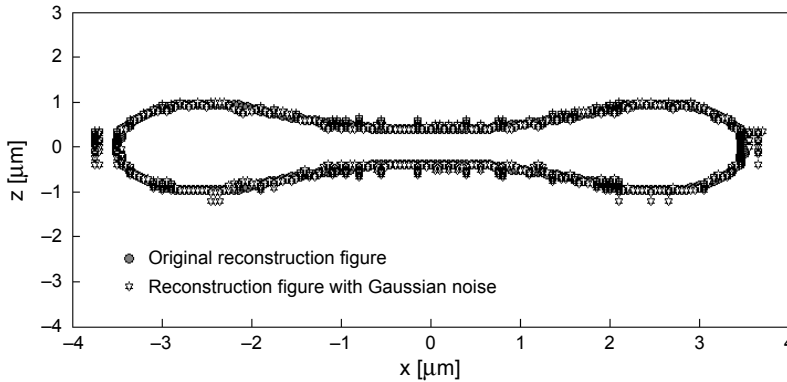
Fig. 7. Collation map of the reconstructed cross-section images between the original reconstructed data and data with Gaussian noise.

In order to study the effect of noise in the reconstruction method, the white Gaussian noise is introduced to the phase images, which is set at 20 dB signal-noise ratio. With the method proposed above, the cellular refractive index distribution data are obtained. The collation map of the cross-section images between the original reconstructed data and those with Gaussian noise is presented in Fig. 7, and it shows that the morphological structure of RBC could be well described with the method proposed in this paper, even with the Gaussian noise.
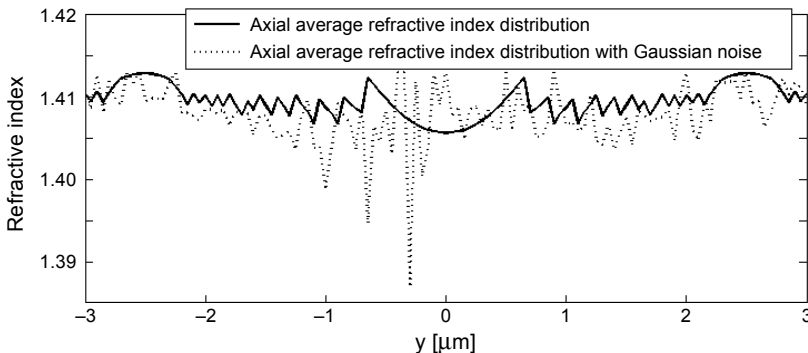

Fig. 8. The axial average refractive index distribution.

According to the phase shift formula, the cellular axial average refractive index (along the z-axis) with the Gaussian noise as well as that without noise is calculated at the same plane as that shown in Fig. 2, which is demonstrated in Fig. 8. From these data, the average refractive indexes of RBC in this plane, with and without the Gaussian noise, are calculated at 1.405 and 1.407, with the relative error at 0.36% and 0.25% compared with the model data of 1.41 respectively. Thus, the validity of the reconstruction under the Gaussian noise could be confirmed by the contrasting results.

4. Conclusion

This paper presents a new method for 3D morphological distribution of the cell. The proposed method inherits the fast convergence and high efficiency of the maximum entropy method, and only two cellular orthogonal quantitative phase images are needed to obtain the spatial refractive index distribution. Thus the 3D morphological distribution of the cell could be reconstructed in detail. The results indicate that the proposed reconstruction method for RBC morphology is effective and feasible. It provides a new way to research the 3D morphological distribution of the biological cell. Meanwhile, the cell model established at the present stage is relatively simple. It is necessary to further refine the model and improve the algorithm as well.

References

[1] Popescu G., *Quantitative Phase Imaging of Cells and Tissues*, McGraw-Hill Professional, 2011.
[2] KyeoReh Lee, Kyoohyun Kim, Jaehwang Jung, JiHan Heo, Sangyeon Cho, Sangyun Lee, Gyuyoung Chang, YoungJu Jo, Hyunjoo Park and YongKeun Park, *Quantitative phase imaging techniques for the study of cell pathophysiology: from principles to applications*, Sensors **13**(4), 2013, pp. 4170–4191.
[3] Marquet P., Rappaz B., Magistretti P.J., Cuche E., Emery Y., Colomb T., Depeursinge C., *Digital holographic microscopy: a noninvasive contrast imaging technique allowing quantitative visualization of living cells with subwavelength axial accuracy*, Optics Letters **30**(5), 2005, pp. 468–470.
[4] Cuche E., Bevilacqua F., Depeursinge C., *Digital holography for quantitative phase-contrast imaging*, Optics Letters **24**(5), 1999, pp. 291–293.
[5] Popescu G., Deflores L.P., Vaughan J.C., Badizadegan K., Iwai H., Dasari R.R., Feld M.S., *Hilbert phase microscopy for investigating fast dynamics in transparent systems*, Optics Letters **29**(21), 2004, pp. 2503–2505.
[6] Ikeda T., Popescu G., Dasari R.R., Feld M.S., *Hilbert phase microscopy for investigating fast dynamics in transparent systems*, Optics Letters **30**(10), 2005, pp. 1165–1167.
[7] Popescu G., Ikeda T., Dasari R.R., Feld M.S., *Diffraction phase microscopy for quantifying cell structure and dynamics*, Optics Letters **31**(6), 2006, pp. 775–777.
[8] YongKeun Park, Diez-Silva M., Popescu G., Lykotrafitis G., Wonshik Choi, Feld M.S., Suresh S., *Refractive index maps and membrane dynamics of human red blood cells parasitized by Plasmodium falciparum*, Proceedings of the National Academy of Sciences of the United States of America **105**(37), 2008, pp. 13730–13735.
[9] Chandramohanadas R., YongKeun Park, Lui L., Ang Li, Quinn D., Liew K., Diez-Silva M., Yongjin Sung, Ming Dao, Chwee Teck Lim, Preiser P.R., Suresh S., *Biophysics of malarial parasite exit from infected erythrocytes*, PLoS ONE **6**, 2011, article e20869.

[10] KYOOHYUN KIM, KYUNG SANG KIM, HYUNJOO PARK, JONG CHUL YE, YONGKEUN PARK, *Real-time visualization of 3-D dynamic microscopic objects using optical diffraction tomography*, Optics Express **21**(26), 2013, pp. 32269–32278.

[11] YOUNGCHAN KIM, HYOEUN SHIM, KYOOHYUN KIM, HYUNJOO PARK, SEONGSOO JANG, YONGKEUN PARK, *Profiling individual human red blood cells using common-path diffraction optical tomography*, Scientific Reports **4**, 2014, article 6659.

[12] LAUER V., *New approach to optical diffraction tomography yielding a vector equation of diffraction tomography and a novel tomographic microscope*, Journal of Microscopy **205**(2), 2002, pp. 165–176.

[13] KYOOHYUN KIM, HYEOK YOON, DIEZ-SILVA M., MING DAO, DASARI R.R., YONGKEUN PARK, *High-resolution three-dimensional imaging of red blood cells parasitized by Plasmodium falciparum and in situ hemozoin crystals using optical diffraction tomography*, Journal of Biomedical Optics **19**(1), 2014, article 011005.

[14] TAEWOO KIM, RENJIE ZHOU, MIR M., DERIN BABACAN S., SCOTT CARNEY P., GODDARD L.L., POPESCU G., *White-light diffraction tomography of unlabelled live cells*, Nature Photonics **8**(3), 2014, pp. 256–263.

[15] KYOOHYUN KIM, ZAHID YAQOOB, KYEOREH LEE, JEON WOONG KANG, YOUNGWOON CHOI, POORYA HOSSEINI, SO P.T.C., YONGKEUN PARK, *Diffraction optical tomography using a quantitative phase imaging unit*, Optics Letters **39**(24), 2014, pp. 6935–6938.

[16] COTTE Y., TOY F., JOURDAIN P., PAVILLON N., BOSS D., MAGISTRETTI P., MARQUET P., DEPEURSINGE C., *Marker-free phase nanoscopy*, Nature Photonics **7**(2), 2013, pp. 113–117.

[17] WONSHIK CHOI, FANG-YEN C., BADIZADEGAN K., SEUNGEUN OH, NIYOM LUE, DASARI R.R., FELD M.S., *Tomographic phase microscopy*, Nature Methods **4**(9), 2007, pp. 717–719.

[18] CHARRIÈRE F., MARIAN A., MONTFORT F., KUEHN J., COLOMB T., CUCHE E., MARQUET P., DEPEURSINGE C., *Cell refractive index tomography by digital holographic microscopy*, Optics Letters **31**(2), 2006, pp. 178–180.

[19] BARBEY N., GUENNOU C., AUCHÈRE F., *TomograPy: a fast, instrument-independent, solar tomography software*, Solar Physics **283**(1), 2013, pp. 227–245.

[20] SHINGYU LEUNG, HONGKAI ZHAO, *A grid based particle method for evolution of open curves and surfaces*, Journal of Computational Physics **228**(20), 2009, pp. 7706–7728.

[21] SHINGYU LEUNG, LOWENGRUB J., HONGKAI ZHAO, *A grid based particle method for solving partial differential equations on evolving surfaces and modeling high order geometrical motion*, Journal of Computational Physics **230**(7), 2011, pp. 2540–2561.

[22] HACKBUSCH W., MITTELMANN H.D., *On multi-grid methods for variational inequalities*, Numerische Mathematik **42**(1), 1983, pp. 65–76.

[23] HACKBUSCH W., *The frequency decomposition multi-grid method*, Numerische Mathematik **56**(2–3), 1989, pp. 229–245.

[24] YONGJIN SUNG, WONSHIK CHOI, FANG-YEN C., BADIZADEGAN K., DASARI R.R., FELD M.S., *Optical diffraction tomography for high resolution live cell imaging*, Optics Express **17**(1), 2009, pp. 266–277.

[25] EIJI NISHIBORI, TADAKATSU OGURA, SHINOBU AOYAGI, MAKOTO SAKATA, *Ab initio structure determination of a pharmaceutical compound, prednisolone succinate, from synchrotron powder data by combination of a genetic algorithm and the maximum entropy method*, Journal of Applied Crystallography **41**(2), 2008, pp. 292–301.

[26] SÖDERBERG K., YOSHIKI KUBOTA, NORIHIRO MUROYAMA, GRÜNER D., ARISA YOSHIMURA, OSAMU TERASAKI, *Electron charge distribution of $CaAl_{2−x}Zn_x$: maximum entropy method combined with Rietveld analysis of high-resolution-synchrotron X-ray powder diffraction data*, Journal of Solid State Chemistry **181**(8), 2008, pp. 1998–2005.

[27] BARDUCCI A., GUZZI D., LASTRI C., MARCOIONNI P., NARDINO V., PIPPI I., *Maximum entropy temperature–emissivity separation in the TIR spectral range using the MaxEnTES algorithm*, Infrared Physics and Technology **56**, 2013, pp. 12–20.

[28] PALMIERI F.A.N., CIUONZO D., *Objective priors from maximum entropy in data classification*, Information Fusion **14**(2), 2013, pp. 186–198.

[29] POPESCU G., YOUNGKEUN PARK, WONSHIK CHOI, DASARI R.R., FELD M.S., KAMRAN BADIZADEGAN, *Imaging red blood cell dynamics by quantitative phase microscopy*, Blood Cells, Molecules and Diseases **41**(1), 2008, pp. 10–16.